Phase quantification in nanobainite via magnetic measurements and X-ray diffraction

Article *in* Journal of Magnetism and Magnetic Materials · November 2014

DOI: 10.1016/j.jmmm.2014.11.037

4 authors:

Wilberth Solano-Alvarez
Arcelor Mittal/ University of Cambridge
21 PUBLICATIONS **355** CITATIONS
SEE PROFILE

Hamilton Abreu
Universidade Federal do Ceará
85 PUBLICATIONS **1,571** CITATIONS
SEE PROFILE

M. R. Silva
Universidade Federal de Itajubá (UNIFEI)
122 PUBLICATIONS **1,613** CITATIONS
SEE PROFILE

Mathew James Peet
University of Cambridge
32 PUBLICATIONS **1,133** CITATIONS
SEE PROFILE

Phase quantification in nanobainite via magnetic measurements and X-ray diffraction

W. Solano-Alvarez[1a], H. F. G. Abreu[b], M. R. da Silva[c], M. J. Peet[a]

[a]*Department of Materials Science and Metallurgy, University of Cambridge, U.K.*

[b]*Departamento de Engenharia Metalúrgica e de Materiais, Universidade Federal do Ceará, Fortaleza, Brazil.*

[c]*Instituto de Física e Química, Universidade Federal de Itajubá, Itajubá, Minas Gerais, Brazil.*

Abstract

Accurate phase quantification of nanostructured bainitic steel is of importance because of the nature of its percolating structure that controls many of its mechanical properties. X-ray diffraction is the technique of choice for such analysis, but magnetic methods can be more rapid and less sensitive to defect structures. In this study, the phase volume fractions measured using both of these techniques for the specific mixtures associated with nanostructured bainite have been compared and contrasted. An expression which relates the volume fraction and the saturation magnetisation is obtained and its form is found to be consistent with previous work done on duplex stainless steels and TRIP steels. The fitting constants used in many of such analyses vary significantly so an attempt is made to rationalise the differences by considering the factors that determine the intrinsic saturation magnetisation of ferrite.

Keywords: nanostructured bainite, phase quantification, saturation magnetisation, X-ray diffraction

[1]E-mail: ws298@cam.ac.uk, Phone: +44 (0) 1223 334336

1. Introduction

Nanostructured bainite contains an extremely fine mixture of ferrite and austenite. The ability of the austenite to percolate the steel dictates amongst other factors, the ductility [1] and its resistance to the diffusion of hydrogen through the two-phase mixture [2]. Given the specific austenite morphology characteristic of nanostructured bainite, there is a critical threshold of austenite fraction below which the material fractures during tensile loading [3], and the austenite also ceases to be effective as a barrier to hydrogen ingress [2].

There are many methods to determine the retained austenite content [4–8], each of which has limitations that have been discussed extensively [9, 10]. Diffraction using X-rays or neutrons has the advantage of rigour in the analysis of data and remains the method of choice for phase fraction analysis. However, magnetic methods to determine volume fractions can be rapid to implement even though they may require calibration. One difficulty is that the calibration constants seem to vary widely as a function of the alloy composition and microstructure [11–16]. In the present work we investigate X-ray diffraction and magnetic detection of retained austenite in nanostructured bainitic steel, and attempt to clarify the nature of the calibration function required for the magnetic technique. Given that there are now several commercial applications and numerous research programmes associated with this structure, it would be useful to have an easy method to characterise the retained austenite content with confidence.

2. Experimental Methods

2.1. Material

All alloys used were cast as 25-50 kg ingots, which were then reduced 50% via hot forging. The chemical compositions are presented in table 1.

2.2. Heat treatments

The heat treatment of small samples cut via electrical-discharge machining included homogenisation at 1200 °C for 2 days and furnace cooling,

Table 1: Chemical composition, wt%, of the alloys used.

Alloy	C	Si	Mn	Cr	Mo	Ni	V	Co	P	S	Al
A	0.79	1.59	1.94	1.33	0.30	0.02	0.11	-	<0.005	-	-
B	0.80	1.59	2.01	1.00	0.24	-	-	1.51	0.002	0.002	-
C	0.79	1.56	1.98	1.01	0.24	-	-	1.51	0.002	0.002	1.01
D	0.78	1.60	2.02	1.01	0.24	-	-	3.87	0.002	0.002	1.37

austenitisation in the γ region (900-1000 ℃) for 15 min and air cooling, bainitic transformation at different temperatures and times (table 2) before being quenched in water at room temperature, and in some cases tempering also for different times and temperatures. For the two heat treatments prior to the bainitic transformation, samples were sealed in quartz tubes back-filled with argon or in a vacuum furnace. Cooling slowly through the 700-550 ℃ range, following homogenisation, was used to ensure pearlite formation and avoid martensite, which would induce quench cracks [17]. Extensive characterisation by X-ray diffraction and microscopy in these and similar conditions has been reported previously [18–22].

The main three parameters that determine the quantity of the ferromagnetic ferrite present are the mass, chemical composition, and the heat treatment of the samples. Therefore, the magnetisation was studied by altering only one of these three parameters at a time in order to separate out their individual contributions. For example, samples 6 and 7 have different compositions but constant heat treatment and approximately constant mass; samples 8, 9 and 10 have different mass but constant composition and heat treatment; samples 3 and 4 have different heat treatment but constant composition and approximately constant mass; and finally samples 1 and 2 have no variation, meaning constant heat treatment, composition, and very similar mass.

2.3. X-ray diffraction

Samples were polished to a 1 µm finish, etched with 2% Nital and analysed with X-ray diffraction (XRD) to measure the volume fractions of bainitic ferrite and retained austenite using a *Philips* PW1830 vertical diffractometer with unfiltered CuK_α radiation. Scans were performed with an acceleration voltage and current of 40 kV and 40 mA from 40 to 125 °, with a step size of

Table 2: Heat treatments performed on different samples. The weight column corresponds to the final sample geometry of thin discs used for TEM and magnetic measurements.

Sample	Alloy	Weight / g	Isothermal transformation		Tempering	
			Temperature / ℃	Time	Temperature / ℃	Time
1	A	0.01135	200	10 days	-	-
2	A	0.01065	200	10 days	-	-
3	A	0.00965	200	10 days	400	1 h
4	A	0.0089	200	10 days	500	1 h
5	B	0.00405	150	1 year	-	-
6	B	0.00395	200	4 days	-	-
7	C	0.0036	200	4 days	-	-
8	D	0.0099	200	4 days	-	-
9	D	0.0064	200	4 days	-	-
10	D	0.01235	200	4 days	-	-

0.05 ° and a dwell time of 26 s. A divergence slit of 0.5 °, an anti-scatter slit of 0.5 °, and a receiving slit of 0.2 mm were used to restrict the beam size and the counts obtained. The volume fractions of ferrite and austenite were derived using *HighScore Plus* and the Rietveld refinement method.

2.4. Transmission electron microscopy

Samples were cut into thin slices 250 µm thick using a silicon carbide cutting wheel and ground down to 40-100 µm using 1200 silicon carbide grinding paper. These thin discs of 0.3 mm in diameter were then electropolished using a twin jet polishing machine and a solution of 80% ethanol, 15% glycerol, and 5% perchloric acid with voltages between 20-40 V. Samples were observed in a JEOL 200 CX with an accelerating voltage of 200 kV.

2.5. Vibrating sample magnetometer

The magnetisation and coercive field of the different samples were measured at room temperature using the TEM discs prior to electropolishing with a VSM EGG-PAR model 4500 with a maximum applied field of 600 kA m^{-1} and total measuring time of 25 min. These conditions were chosen in order to be able to compare the results to XRD volume fractions and to other magnetic measurements in the literature, which were mostly performed at room temperature. This study concentrates only on dual phase systems, but

it should be noted that for the tempered samples additional measurements could be performed above the Curie temperature of cementite (480 K) without affecting the structure in order to obtain information about the carbide phase fractions.

3. Results and discussion

Given the similarity in heat treatments and expected nanostructure, only some representative samples were studied using TEM. The images obtained are presented in fig. 1. For the sake of brevity, samples from here onwards are referred to as X-$T^{isotrans}$-$t^{isotrans}$-T^{temper}-t^{temper}-Y, where X is the alloy type, T stands for the temperature in [℃], t is the time in hours [h], days [d], or years [y], and Y is the sample number in case of there being more than one with the same composition and heat treatment.

The stereologically corrected bainitic plate size of some untempered samples was determined using the mean width in the direction normal to the plate length. For sample 1 (A-200C-10d-1) and 2 (A-200C-10d-2) the mean thickness is 39±1 nm and for sample 5 (B-150C-1y) it is 51±4 nm [18].

The volume fraction of retained austenite obtained via Rietveld analysis of the complete XRD spectra (including overlapping peaks) is presented in table 3 along with the values of saturation magnetisation per unit mass obtained at the maximum applied field and the effective field corrected by the demagnetisation factor corresponding to shape (thickness) of each sample [23]. The magnetisation curves are presented in fig. 2.

It can be seen from table 3 that tempering at 500 ℃ for 1 h decomposed all the retained austenite and left behind a completely ferritic structure, as confirmed by the TEM image of fig. 1b. It is therefore not surprising that this sample displayed the highest specific saturation magnetisation. By plotting the measured volume fraction of bainitic ferrite V_{α_b} against the specific saturation magnetisation m_s (fig. 3), it was possible to perform a linear fit which yields the following equation

$$V_{\alpha_b} \;=\; 0.0054\, m_s - 0.015 \tag{1}$$

The small value of the y-intercept confirms the fact that the magnetisation of a completely austenitic sample should be approximately zero [14], so the

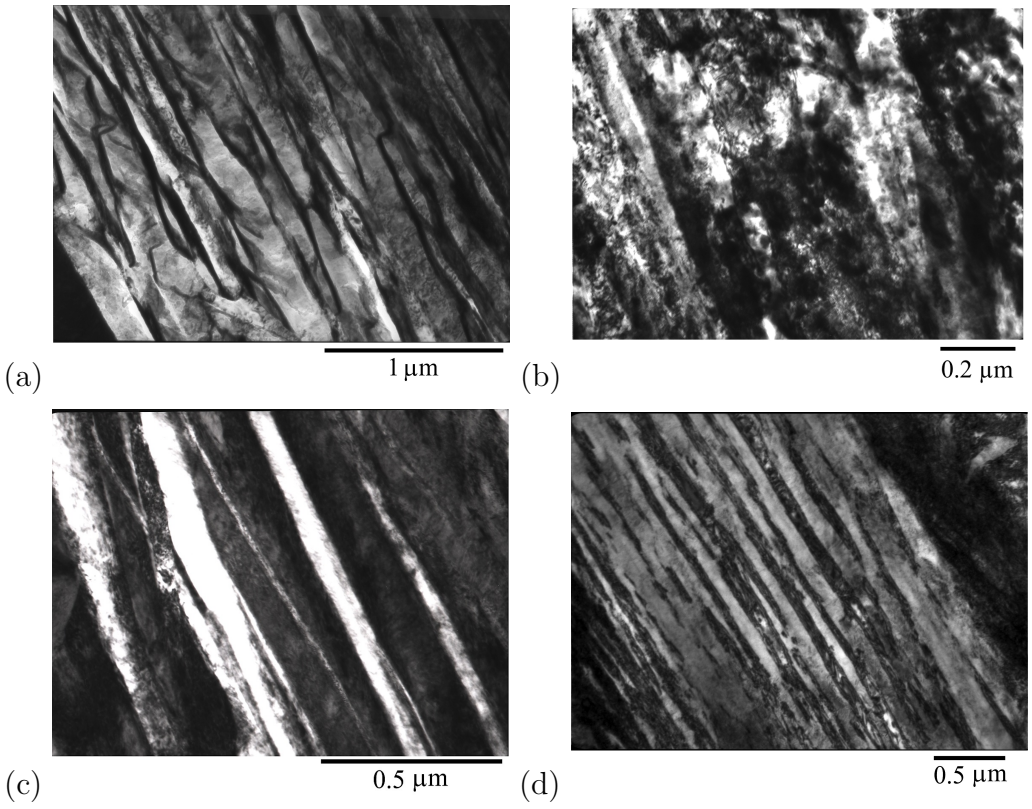

(a) (b) (c) (d)

Figure 1: TEM micrographs of samples: a) 3 (A-200C-10d-400C-1h), b) 4 (A-200C-10d-500C-1h), c) 5 (B-150C-1y), and d) 8 (D-200C-4d-1).

Table 3: Volume fraction of retained austenite V_γ, saturation magnetisation m_s, and effective field H_{eff} for each sample. The error to all volume fractions is ± 0.01 and for all magnetisation measurements, ± 1 . For the analysis, only bainitic ferrite and austenite were considered, although the structure will contain carbides after tempering.

Sample	V_γ	m_s / A m^2 kg^{-1}	H_{eff} / kA m^{-1}
1 A-200C-10d-1	0.215	149.4	167.6
2 A-200C-10d-2	0.215	149.2	168
3 A-200C-10d-400C-1h	0.161	152.7	168.5
4 A-200C-10d-500C-1h	0	184.9	167.6
5 B-150C-1y	0.204	154.3	172.1
6 B-200C-4d	0.192	145.5	172.3
7 C-200C-4d	0.171	163.1	172.3
8 D-200C-4d-1	0.233	147.7	168.5
9 D-200C-4d-2	0.233	150.1	170.7
10 D-200C-4d-3	0.233	143.0	167.3

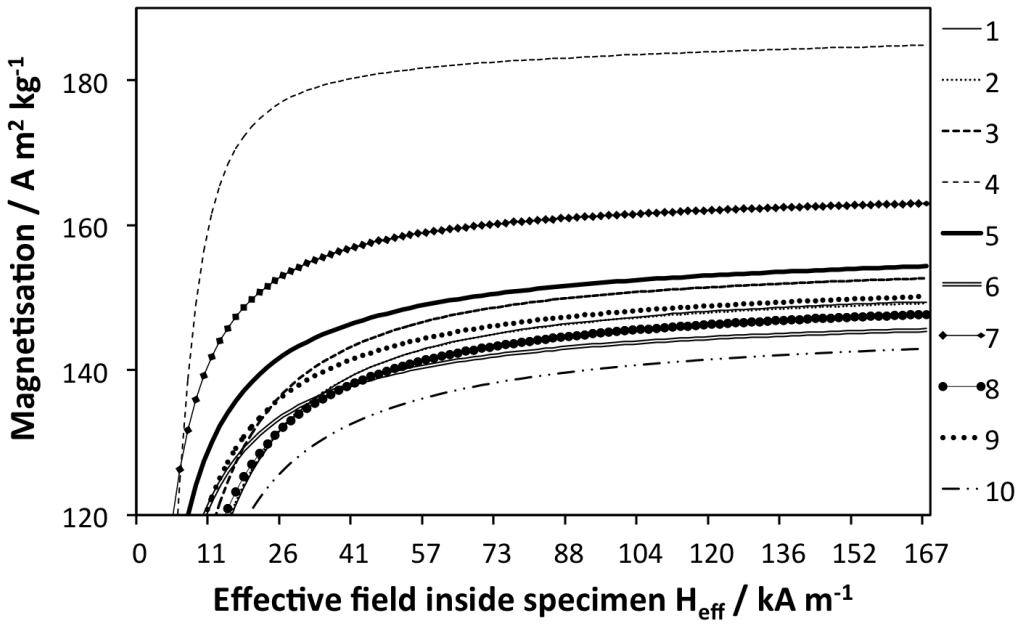

Figure 2: Magnetisation curves for each sample.

equation can be rewritten as

$$V_{\alpha_b} = \frac{m_s}{185.2} \tag{2}$$

The value $185.2\,\mathrm{A\,m^2\,kg^{-1}}$ represents the intrinsic saturation magnetisation of ferrite (M_s) with a average of the compositions in table 1, which is in close agreement with the measured magnetisation of $184.9\,\mathrm{A\,m^2\,kg^{-1}}$ for sample 4 (A-200C-10d-500C-1h).

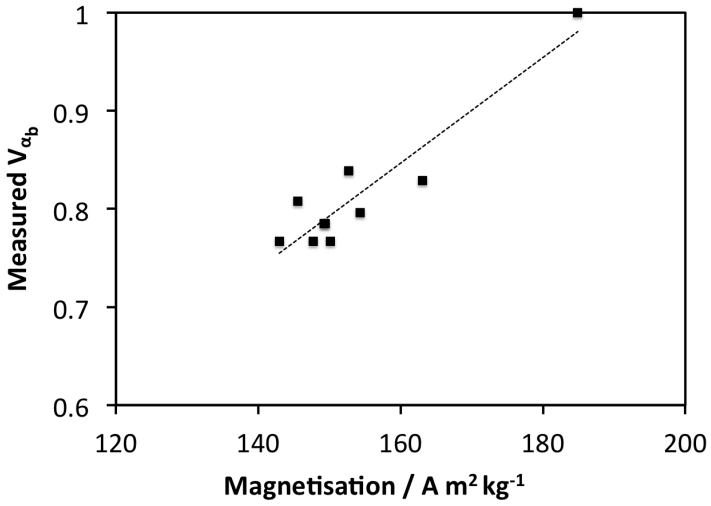

Figure 3: Measured volume fraction of bainitic ferrite and saturation magnetisation.

By using equation 2, it is possible to plot the expected volume fraction of bainitic ferrite for all samples against the measured value. As seen in fig. 4, 70% of the measured values lie within the error bars of the calculated value despite slight compositional variations. The error bars of the measured values all correspond to 0.01 given by the generally achieved accuracy of the Rietveld refinement method using *High Score Plus*, whilst the error bars of the calculated values were determined by

$$\delta V_{\alpha_b} = 0.005423\,\delta m_s + 0.000137\,m_s \tag{3}$$

where 0.005423 is the average of the V_{α_b}/m_s ratio of all samples and 0.000137 is its standard error, as described in [14].

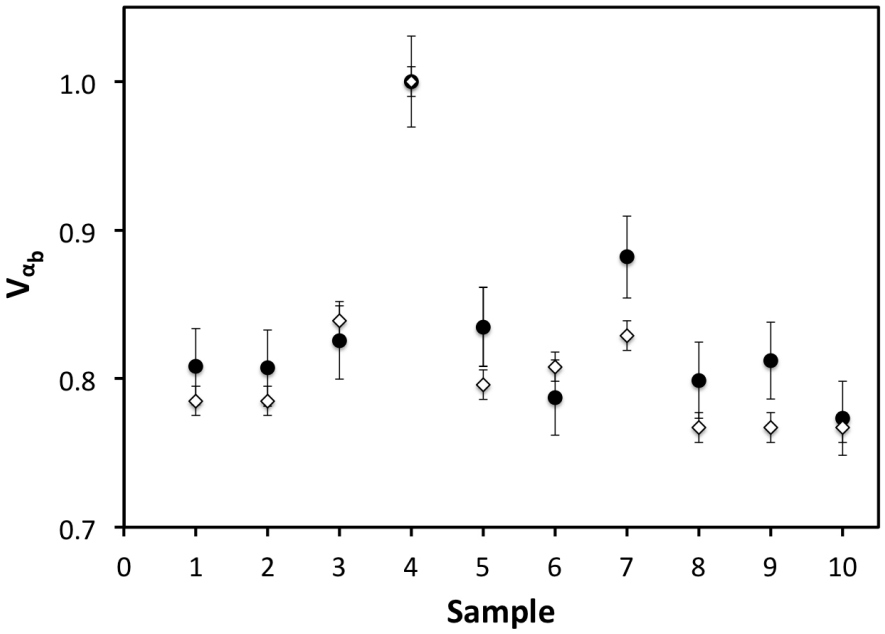

Figure 4: Measured volume fraction of ferrite via diffraction (black dots) compared with the calculated value (white diamond) using the proposed equation.

The fact that the ferrite volume fraction of sample 5 (B-150C-1y), 7 (C-200C-4d) and 9 (D-200C-4d-2) cannot be accurately predicted is not clear as it could not be attributed to either the mass of the sample, the chemical composition, or the heat treatment. It is possible nevertheless that since magnetic measurements were performed on TEM samples, the nanostructure was not homogenous for such sample size or there was stress induced transformation of the retained austenite to martensite. Recent research has shown that even after significant cycling stressing, the austenite films of nanostructured bainite in the regions of maximum subsurface shear stress do not stress transform to martensite [24]. Nevertheless, less stable blocky austenite regions could in principle transform to martensite during thin disc sample preparation distorting volume fraction measurements. Ion milling of the samples would reduce this effect, but given the cost and time associated with it, standard TEM sample preparation was chosen knowing that the affected region caused by the final grinding step with 1200 grit is $\sim$26 µm for both sides, which corresponds to $\sim$10-40% of the sample volume depending on the different specimen thickness. Analysis of samples 8, 9, and 10 that have the same composition and heat treatment but different thickness (178, 155, and 222 µm respectively) confirms that the thinnest sample has the highest magnetisation and thus the highest ferrite content (150.1 A m^2 kg^{-1}) and the thickest one, the lowest (143.0 A m^2 kg^{-1}) that could in part be because the region of possible stress transformation of austenite to martensite is a larger percentage of the whole sample. Although sample preparation is a variable that could lead to further improvement of the accuracy of magnetic phase quantification, the different magnetisation values for samples 8-10 still lie within the error estimated.

A variety of values have been found for the intrinsic saturation magnetisation of ferrite in different steels (saturation magnetisation of samples containing virtually no austenite), but no quantitative explanations of such difference have been presented in the literature to date. Here, a simple calculation was performed to estimate this quantity based solely on the chemical composition of the alloy

$$M_s^{\mathrm{calc}} = k\frac{\sum m_s^i x_i}{\sum x_i} \tag{4}$$

Since only iron (m_s^{Fe}=218 A m^2 kg^{-1}), cobalt (m_s^{Co}=159 A m^2 kg^{-1}), and nickel (m_s^{Ni}=54.4 A m^2 kg^{-1}) are ferromagnetic at room temperature, m_s for all

other elements was taken as $0\,\mathrm{A\,m^2\,kg^{-1}}$ [25]. x is the weight percent of each element and k is a correction factor that will be discussed later. The results of this calculation for different alloys in contrast with the measured values are presented in table 4.

Table 4: Measured (M_s^{exp}) and calculated (M_s^{calc}) intrinsic saturation magnetisation of ferrite for different alloys, except for the ones marked with † which are martensitic. Magnetic measurements were performed at room temperature (temperature not stated in those marked with *). The chemical composition of each alloy is shown in wt%.

Name	M_s^{exp} / $\mathrm{A\,m^2\,kg^{-1}}$	M_s^{calc} / $\mathrm{A\,m^2\,kg^{-1}}$	Fe	C	Si	Mn	Cr	Mo	Ni	V	Co	P	S	N	Nb	Ti	Al
Superduplex stainless UNS S32750 [14]	128	142.1	63.523	0.02	0.34	0.83	24.57	3.75	6.68	-	-	0.026	0.001	0.26	-	-	-
Duplex stainless UNS S39205 [13]	133*	154.5	69.575	0.032	-	-	22.38	2.55	5.32	-	-	0.028	0.003	0.1123	-	-	-
304 stainless [26]	160.4* †	160.2	71.299	0.07	0.72	1.32	18.03	-	8.46	-	0.08	0.015	0.006	-	-	-	-
Superbainite (Alloy A)	184.9	204.7	93.915	0.79	1.59	1.94	1.33	0.30	0.02	0.11	-	0.005	-	-	-	-	-
300 maraging steel [16]	188	170.4	66.93	0.01	-	-	-	4.96	17.86	-	9.31	-	-	-	-	0.79	0.14
TRIP (Al1.4P) [12]	189.5	211.2	96.87	0.18	0.02	1.52	-	-	-	-	-	0.005	-	0.004	-	-	1.4
TRIP (Al1.8) [12]	197.5	210.1	96.36	0.2	0.02	1.53	-	-	-	-	-	0.081	-	0.0055	-	-	1.8
Cr- High carbon [15]	206.4 †	212.1	97.3	0.93	0.21	0.69	0.68	0.14	-	-	-	0.013	0.004	-	0.032	-	-

In fig. 5, the calculated values of intrinsic saturation magnetisation for each of the alloys in table 4 are plotted against the measured experimental values. A linear regression was applied which yielded the following equation if solved for M_s^{exp}

$$M_s^{\mathrm{exp}} = 1.13 M_s^{\mathrm{calc}} - 33.35 \tag{5}$$

In previous work it is assumed that the chemical composition dominates the intrinsic saturation magnetisation of the ferrite, while it is acknowledged that microstructure also plays a role [12, 15, 27]. From our analysis it is possible to quantify how dominant the chemical composition actually is. Given the significant grain size difference between samples such as nanostructured bainite with a mean ferritic plate size of ∼40-60 nm and the superduplex stainless steel with grains up to ∼350 µm, it can be speculated that there must be a contribution of the ferritic grain size (domain size), shape/size of the sample[2], and crystal structure of the ferritic phase (cubic or tetragonal) that can be incorporated to equation 4 by a constant k, which has a value of 1.052 for this study if the linear regression is performed with an intercept of zero. By providing data such as the grain and sample size in future studies, a more complete equation to predict the intrinsic saturation magnetisation

[2]Zhao et al. measured a 3% difference in the saturation magnetisation between small and large samples [12].

of ferrite, M_s, and hence the volume fraction of ferrite/austenite could, in principle, be determined using magnetic measurements alone.

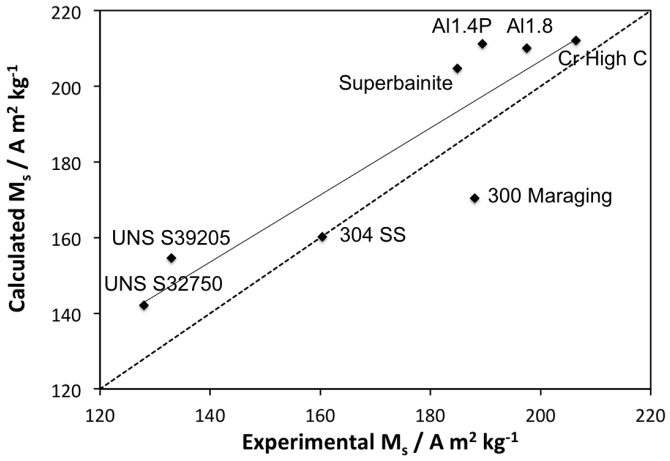

Figure 5: Calculated intrinsic saturation magnetisation against experimental values for different alloys. The continuous line is the applied linear regression and the dashed line represents perfect correspondence to the experimental data.

4. Conclusion

By performing a short magnetisation measurement at room temperature it is possible to confidently determine the amount of austenite/ferrite volume fraction of a nanostructured bainitic alloy irrespective of small compositional variations by using $V_{\alpha_b} = m_s/185.2$. Similar expressions have been derived for stainless steels with substantial compositional, grain size, and phase volume fraction differences confirming the applicability of magnetisation measurements as a reliable tool for phase quantification in steels.

A simple calculation has been performed to determine the intrinsic saturation magnetisation of ferrite based solely on the chemical composition of the ferromagnetic elements present in the alloy. The results indicate that chemical composition does not predict this property entirely and that additional parameters such as the grain size (domain size), sample size/shape, or crystal structure of the ferrite may need to be considered in the development of a generally applicable model.

5. Acknowledgements

Funding by CONACyT, the Cambridge Overseas Trust, and the Roberto Rocca Education Programme is highly appreciated and acknowledged. We are very thankful to Prof. H. K. D. H. Bhadeshia and Dr. Ting Ping Hou for comments, suggestions, and encouragement.

6. References

[1] H. K. D. H. Bhadeshia, Properties of fine–grained steels generated by displacive transformation, Materials Science and Engineering A 481–482 (2008) 36–39.

[2] L. C. D. Fielding, E. J. Song, D. K. Han, H. K. D. H. Bhadeshia, D. W. Suh, Hydrogen diffusion and the percolation of austenite in nanostructured bainitic steel, Proceedings of the Royal Society of London A 470 (2014) 20140108.

[3] M. Sherif, C. Garcia-Mateo, T. Sourmail, H. K. D. H. Bhadeshia, Stability of retained austenite in TRIP–assisted steels, Materials Science and Technology 20 (3) (2004) 319–322.

[4] M. J. Dickson, Significance of texture parameters in phase analysis by X-ray diffraction, Journal of Applied Crystallography 2 (1969) 176–180.

[5] R. L. Bannerjee, X-ray determination of retained austenite, Journal of Heat Treating 2 (1981) 147–150.

[6] J. X. Zhang, P. M. Kelly, L. K. Bekessy, J. D. Gates, Determination of retained austenite using an X-ray texture goniometer, Materials Characterization 45 (2000) 39–49.

[7] M. Radu, J. Valy, A. F. Gourgues, F. L. Strat, A. Pineau, Continuous magnetic method for quantitative monitoring of martensitic transformation in steels containing metastable austenite, Scripta Materialia 52 (2005) 525–530.

[8] L. K. Perry, D. H. Ryan, R. Gagon, Studying surfaces and thin films using mössbauer spectroscopy, Hyperfine Interactions 170 (2006) 131–143.

[9] J. Talonen, P. Aspergren, H. Hänninen, Comparison of different methods for measuring strain induced martensite content in austenitic steels, Materials Science and Technology 20 (2004) 1506–1512.

[10] P. J. Jacques, S. Allain, O. Bouaziz, A. De, A. F. Gourgues, B. M. Hance, Y. Houbaert, J. Huang, A. Iza-Mendia, S. E. Kruger, M. Radu, L. Samek, J. Speer, L. Zhao, S. van der Zwaag, On measurement of retained austenite in multiphase TRIP steels — results of blind round robin test involving six different techniques, Materials Science and Technology 25 (2009) 567–574.

[11] L. Zhao, N. H. van Dijk, A. J. Lefering, J. Sietsma, Magnetic detection of small fractions of ferromagnetic martensite within the paramagnetic austenite matrix of TWIP steel, Journal of Materials Science 48 (4) (2013) 1474–1479.

[12] L. Zhao, N. H. V. Dijk, E. Brück, J. Sietsma, S. V. der Zwaag, Magnetic and X-ray diffraction measurements for the determination of retained austenite in trip steels, Materials Science and Engineering A 313 (1) (2001) 145–152.

[13] S. S. M. Tavares, P. D. S. Pedrosa, J. R. Teodosio, M. R. D. Silva, J. M. Neto, S. Pairis, Magnetic properties of the UNS S39205 duplex stainless steel, Journal of alloys and compounds 351 (1) (2003) 283–288.

[14] S. S. M. Tavares, J. M. Pardal, J. A. D. Souza, J. M. Neto, M. R. D. Silva, Magnetic phase quantification of the UNS S32750 superduplex stainless steel, Journal of Alloys and Compounds 416 (1) (2006) 179–182.

[15] S. S. M. Tavares, S. R. Mello, A. M. Gomes, J. M. Neto, M. R. D. Silva, J. M. Pardal, X-ray diffraction and magnetic characterization of the retained austenite in a chromium alloyed high carbon steel, Journal of Materials Science 41 (15) (2006) 4732–4736.

[16] J. M. Pardal, S. S. M. Tavares, M. C. Fonseca, M. R. da Silva, J. M. Neto, H. F. G. Abreu, Influence of temperature and aging time on hardness and magnetic properties of the maraging steel grade 300, Journal of Materials Science 42 (7) (2007) 2276–2281.

[17] W. Solano-Alvarez, H. K. D. H. Bhadeshia, Controlled-cracking of bearing steel: part 1, Metallurgical & Materials Transactions A 45 (2014) DOI: 10.1007/s11661–014–2430–y.

[18] M. J. Peet, Transformation and tempering of low temperature bainite, Ph.D. thesis, University of Cambridge (2010).

[19] C. Garcia-Mateo, F. G. Caballero, H. K. D. H. Bhadeshia, Acceleration of low–temperature bainite, ISIJ International 43 (2003) 1821–1825.

[20] C. Garcia-Mateo, M. Peet, F. G. Caballero, H. K. D. H. Bhadeshia, Tempering of a hard mixture of bainitic ferrite and austenite, Materials Science and Technology 20 (2004) 814–818.

[21] H. J. Stone, M. J. Peet, H. K. D. H. Bhadeshia, P. J. Withers, S. S. Babu, E. D. Specht, Synchrotron X-ray studies of austenite and bainitic ferrite, Proceedings of the Royal Society A 464 (2008) 1009–1027.

[22] H. S. Hasan, M. J. Peet, M.-N. Avettand-Fènoël, H. K. D. H. Bhadeshia, Effect of tempering upon the tensile properties of a nanostructured bainitic steel, Materials Science and Engineering A 615 (2014) 340–347.

[23] B. D. Cullity, C. D. Graham, Introduction to Magnetic Materials, Addison–Wesley Publication Company, Reading, Mass., 1972.

[24] W. Solano-Alvarez, E. J. Pickering, H. K. D. H. Bhadeshia, Degradation of nanostructured bainite under rolling contact fatigue, Materials Science & Engineering A 617 (2014) 156–164.

[25] C. M. Sorensen, Magnetism in Nanoscale Materials in Chemistry, John Wiley and Sons, Inc., New York, USA, 2002.

[26] P. L. Mangonon, G. Thomas, Structure and properties of thermal-mechanically treated 304 stainless steel, Metallurgical transactions 1 (6) (1970) 1587–1594.

[27] S. S. M. Tavares, M. R. D. Silva, J. M. Pardal, H. F. G. Abreu, A. M. Gomes, Microstructural changes produced by plastic deformation in the UNS S31803 duplex stainless steel, Journal of Materials Processing Technology 180 (1) (2006) 318–322.